DOI: 10.1002/adma.200702380

Sequence-Dependent Fluorescence of DNA-Hosted Silver Nanoclusters**

By *Elisabeth G. Gwinn*,* *Patrick O'Neill*, *Anthony J. Guerrero*, *Dave Bouwmeester*, and *Deborah Kuchnir Fygenson*

Artificial structures built from synthetic DNA are emerging as platforms for device science that offer greatly enhanced resolution and simplicity of fabrication compared to traditional solid-state structures. These advantages arise from the nanometer-scale control over geometry provided by aqueous self-assembly of designed DNA sequences, which yields robust "scaffolds" in a palette of nanometer-scale geometries ranging from octahedra to two-dimensional lattices of all types. [1–10] Future applications that arise from such DNA scaffolds may include nanometer-scale optics, nanometer-scale electronics, and single-molecule detection proteomics.[2]

Realizing the promise that DNA-based materials hold for nanometer-scale device science will require the development of functional nanoelements for patterning of DNA scaffolds. In analogy to the layout of logic and memory elements on a semiconductor chip, nanoelements with properties that can be varied in a controlled manner across the underlying scaffold are needed. Such nanoelements should have lateral dimensions no larger than a few nanometers, in order to take advantage of the ultrafine, 6 nm resolution currently available in DNA scaffolds.[10] Nanoelements should be hosted within DNA strands that can integrate into the scaffold structure, to enable precise positioning. Finally, nanoelement properties should depend on the base sequence of their host DNA strand, to provide site-specific behavior. Such a combination of properties would increase flexibility and function in comparison to current approaches for patterning DNA scaffolds with attachments, such as Au nanoparticles[3,4] and proteins,[5–7] which are relatively bulky and lack sensitivity to the sequence of nearby DNA bases.

Here we show that silver nanoclusters bound to short, synthetic DNA strands provide optically functional nanoelements with the desired small size, sequence sensitivity, and suitability for integration into DNA scaffolds. Our work builds on the initial discovery of fluorescence from few-atom silver clusters attached to a 12-base, single-stranded DNA sequence.[11] We use six 19-base DNA oligomers to show that visibly fluorescent silver clusters form only in single-stranded regions of the DNA hosts. This selectivity opens the possibility of precise positioning of optical nanoelements on DNA scaffolds through use of DNA "hairpin" sequences, which have already been used to create patterns of high complexity, with resolution below 10 nm, upon double-stranded DNA scaffolds.[10] We find that the spectral characteristics of these silver-DNA nanoelements can be controlled by the base sequence and secondary structure of the DNA strands that host the silver atoms, a result that may ultimately contribute to achieving sequence-programmed optical addressing with nanometer-scale resolution.

Scheme 1 represents the oligomers studied here.[14] Colored circles indicate the bases: blue = cytosine (C), green = thymine (T), red = guanine (G), and yellow = adenine (A). C-Strand and G-Strand are complementary sequences that, alone in solution, are each predominantly single-stranded (ss), but form a purely double-stranded (ds) "Duplex" when thermally annealed together under our solution conditions. The hairpin oligomers C-loop, G-loop, A-loop and T-loop are partially self-complementary sequences with a common, 7-base

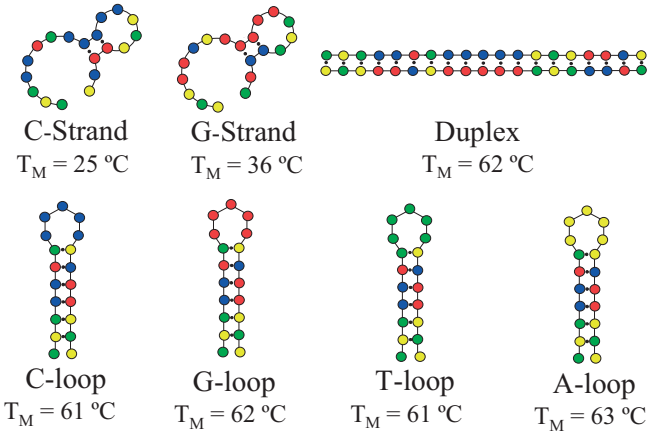

Scheme 1. Cartoons of the 19-base DNA oligomers used in this work. Blue = cytosine (C), green = thymine (T), red = guanine (G), and yellow = adenine (A). Black dots represent base pairing and solid lines the sugar-phosphate backbone. The T_M are calculated values [12] that agree with measured hairpin melting temperatures [13]. Top: C-Strand and G-Strand form the Duplex when annealed together. Bottom: Hairpins C-loop, G-loop, T-loop and A-loop.

[*] Prof. E. G. Gwinn, P. O'Neill, A. J. Guerrero, Prof. D. Bouwmeester, Prof. D. K. Fygenson
Physics Department and California Nanosystems Institute
University of California
Santa Barbara, CA 93106 (USA)
E-mail: bgwinn@physics.ucsb.edu
Prof. D. K. Fygenson
Biomolecular Science and Engineering Program
University of California
Santa Barbara, CA 93106 (USA)

[**] Supported by a UCSB Academic seed grant (E.G.) and by NSF-CCF-622257 (D.B. and D.K.F.). P.O'N. acknowledges support as a GK-12 Fellow (NSF-DGE-0440576). Supporting Information is available online from Wiley InterScience or from the authors.

ADVANCED MATERIALS

pair stem that closes a single-stranded loop, roughly 2 nm across, that is composed of five identical bases. The C-rich sequences C-loop and C-Strand differ only in the reversal of the order of the seven bases on the 3' ends of the sequences.[14] The G-rich sequences G-loop and G-Strand differ only in the reversal of the order of the seven bases on their 5' ends.[14] The hairpins have measured melting temperatures,[13] T_M, near 60 °C, in good agreement with calculated values[12] that also give T_M near 60 °C for the Duplex, and much lower T_M for C-Strand and G-Strand (25 °C and 36 °C, respectively). Thus, at room temperature, the double-stranded stem firmly closes the hairpins, the Duplex is expected to have no single-stranded regions, and C-Strand and G- Strand are expected to have just two, barely bound base pairs.

To synthesize optically functional Ag-DNA nanoelements, we added $AgNO_3$ to DNA strands hydrated in ammonium acetate, followed by reduction with $NaBH_4$. Final concentrations were 25 μM in each DNA strand,[15] 140 μM in $AgNO_3$ (5.6 Ag/strand), 280 μM in $NaBH_4$, and 40 mM in ammonium acetate at pH 6.9.

For all of the oligomers, the reduced solutions were pale yellow to the eye and fluorescent. Fluorescence was not observed in the absence of DNA, nor in solutions of DNA without $AgNO_3$, nor in unreduced $AgNO_3$-DNA solutions. The yellow color, but no fluorescence, was observed when Ag reduction by $NaBH_4$ was performed in the absence of DNA, and is characteristic of surface plasmon absorption by silver nanoparticles 10–50 nm in diameter.[16] Thus DNA-Ag nanoclusters produced the observed fluorescence, and the much larger Ag nanoparticles also present in solution contributed only to the visible absorption.

The intensity of the fluorescence from the DNA-Ag solutions increased gradually over roughly 24 hours after reduction by $NaBH_4$, and decayed slowly thereafter over a period of days to several weeks, depending on sequence (presumably due to oxidation of Ag clusters). Fluorescence data shown here were therefore collected 22–26 hours after reduction. Relative fluorescence intensities of the different DNA-Ag solutions were similar at 5, 10, and 24 hours post-reduction; thus the time-evolution of the fluorescence is similar in all cases and the differences in fluorescence properties shown below are characteristic of the oligomer sequences.

To characterize the number of silver atoms in the Ag-DNA species, we collected time-of-flight mass spectra (electrospray ionization). Figure 1 shows the data over the range of mass to charge ratio, M/Z, that spans the dominant charge state. The spectra are normalized by the integral of the signal over the displayed range of M/Z, and were collected roughly 20 hours after addition of $NaBH_4$. The dominant charge state was $Z = -4$ for all oligomers under the conditions used, except for the Duplex, for which the $Z = -7$ charge state had the highest signal. Relative abundances were similar for other values of Z. Mass spectra of the hairpin solutions exhibited peaks for the monomer strands only,[17] as expected for the DNA concentrations used here.

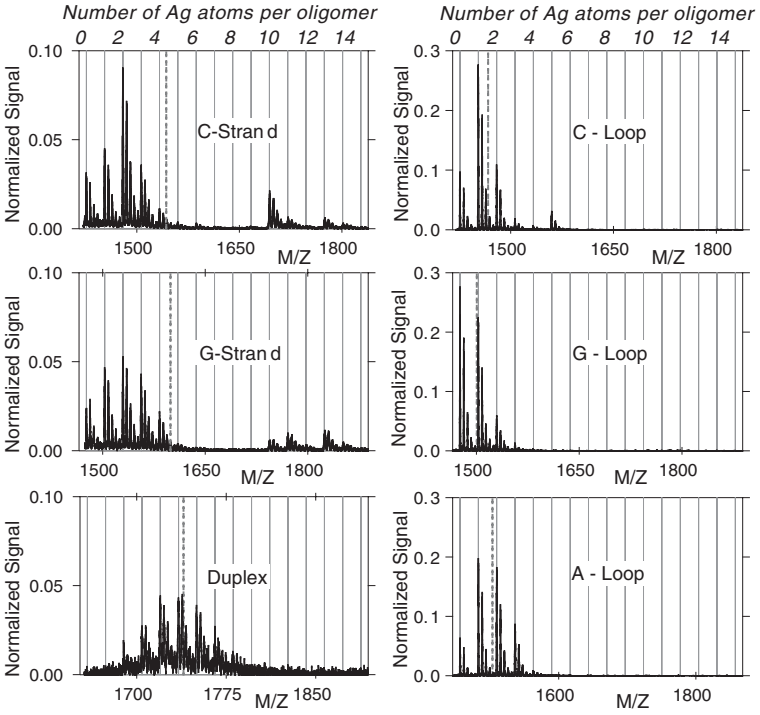

Figure 1. Mass spectra of the DNA-Ag solutions, for (left column) C-Strand, G-Strand, and Duplex, and (right column) C-loop, G-loop, and A-loop. The mass spectrum produced by T-loop (Supporting Information) is similar to that for A-loop. Spectra are normalized by the integral of the signal over the displayed range. Gray lines mark the M/Z corresponding to attachment of N_{Ag} = 0, 1, 2, ... Ag atoms. Dashed lines: average number of Ag atoms per strand, $<N_{Ag}>$.

In Figure 1, vertical, gray lines mark peaks corresponding to oligomers with N_{Ag} = 0, 1, 2 ... attached silver atoms. The closely spaced peaks at slightly greater M/Z correspond to the additional attachment of 1, 2, 3... sodium atoms. Dashed lines indicate the average number of attached Ag atoms, $<N_{Ag}>$.

All of the oligomers bind Ag atoms, as shown in Figure 1 (Supporting Information shows the mass spectrum of T-loop). Because previous studies of the binding of Ag cations to DNA found no detectable interaction of Ag^+ with phosphate groups,[18] we expect that Ag atoms are bound only to the bases. All of the oligomers exhibit $<N_{Ag}>$ below 5.6, the number of silver ions added per oligomer and per Duplex. This is as expected from the coexistence with the DNA-bound nanoclusters of much larger, non-fluorescent Ag nanoparticles that compete for the Ag.

We find that strikingly different fluorescence spectra result from using the different oligomers as hosts for Ag. Figure 2 shows the fluorescence intensity as contour maps in the excitation (λ_{ex})–emission wavelength (λ_{em}) plane. The wavelengths displayed capture the dominant spectral features detected for excitation at visible wavelengths, λ_{ex}, fixed every 10 nm in the range 400–700 nm (Supporting Information shows individual spectra). In all plots, the black contour lies at

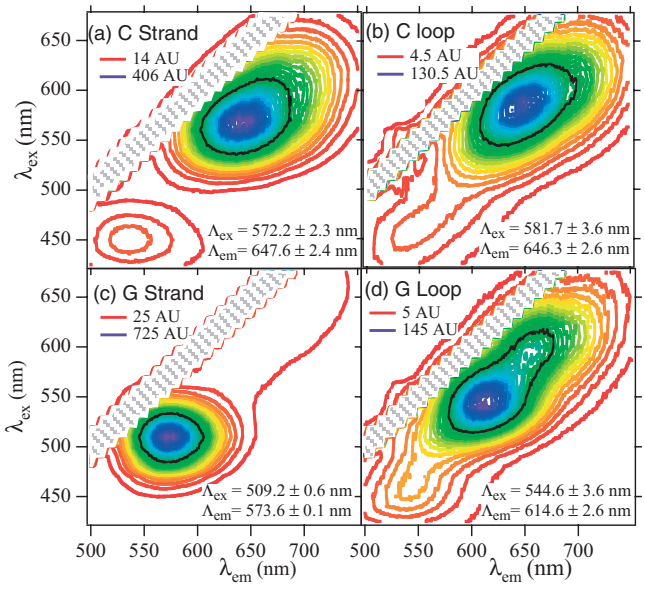

Figure 2. Contour maps of fluorescence from DNA-Ag solutions. The black contour lies at half the maximum intensity. *Upper legend*: contour interval and peak intensity. *Lower legend*: wavelengths of the primary peak, derived from three independent data sets. Shaded regions along $\lambda_{ex} = \lambda_{em}$: scattered light prevents detection of fluorescence. a) C-Strand. b) G-Strand. c) C-loop. d) G-loop.

half the peak signal, the contour interval is 1/29 of the peak signal, and the upper legend indicates the peak intensity (purple) and base contour (red).

Both C-Strand and G-Strand produce brightly fluorescent DNA-Ag solutions (Fig. 2a and c), However, despite the presence of attached Ag (Fig. 1), the Duplex produces negligible visible fluorescence (Supporting Information). Apparently the mode of binding of Ag to dsDNA yields electronic configurations without excitations in the visible or/and that undergo rapid non-radiative decay. We expect that the primary locations for silver attachment to the Duplex are the N7 sites of the guanine bases, based on previous studies of the binding of Ag to ds DNA.[18] The guanine N7 site is not involved in base pairing between strands.

Because the constituent, C- and G-Strands of the Duplex each host fluorescent Ag species (Fig. 2a and c), while the Duplex does not, we conclude that Ag atoms bind to single-stranded DNA via sites that are rendered inaccessible by Watson–Crick base pairing. Different modes of binding of Ag to ssDNA and to dsDNA are also suggested by the qualitative differences between the mass spectrum of the Duplex and those of C- and G-Strand (Fig. 2): the single strands exhibit bimodal mass spectra with low N_{Ag} (0–4) and with high N_{Ag} (10–14) components, while the Duplex mass spectrum exhibits only intermediate N_{Ag}. Studies of silver bound to other organic molecules with high densities of amine and/or carbonyl oxygen sites, such as dendrimers,[19] polymer microgels,[20] and molecular polygels,[21] have also observed fluorescent Ag species. We infer that carbonyl oxygen and/or amine groups participate in binding Ag to bases on ssDNA.

The main fluorescence peaks for C- and G-Strands (Fig. 2a and c) are much stronger than all satellite features, suggesting a predominant emissive species that interacts with a fluctuating environment. The fluorescence spectral features are highly reproducible over repeated syntheses. The lower legends in Figure 2 specify the excitation and emission wavelengths, Λ_{ex} and Λ_{em}, that correspond to the maximum fluorescence intensity. We found Λ_{ex} and Λ_{em} from Gaussian fits to three independent data sets taken on solutions synthesized from separate batches of the DNA. The peak excitation and emission wavelengths for G-Strand were constant to within 1 nm among data sets (lower legend, Fig. 2c); while for C-Strand they were constant to within 3 nm (Fig. 2a).

The primary fluorescence peaks produced by C- and G-Strands lie at distinct wavelengths: Λ_{ex} = (572.2 ± 2.3) nm, Λ_{em} = (647.6 ± 2.4) nm and Λ_{ex} = (509.2 ± 0.6) nm, Λ_{em} = (573.6 ± 0.1) nm, respectively. We conclude that the fluorescence spectrum generated by ssDNA hosts depends on the base sequence, as originally proposed in reference [11]. The similar fluorescence intensities produced by C- and G-Strand ((363 ± 90) AU and (622 ± 96) AU, respectively, averaged over three data sets) and their similar mass spectra (Fig. 1) indicate that Ag binds with comparable affinities to chemically similar sites on C and G bases at neutral pH. The different peak wavelengths in the fluorescence spectra then reflect differences in local environment provided by the different base stacking interactions within the two strands. The apparent similarity in binding affinities of Ag for single-stranded G and C differs from the interpretation of previous studies[11] of Ag bound to a 12-base oligomer, 5'-AGGTCGCCGCCC-3', which used NMR to identify cytosine as the main site for Ag attachment; however, because the solutions studied had roughly 40 times higher concentrations than used here, the dominant mode of Ag binding may have been different.[18]

To improve understanding of the relationship between DNA sequence and the spectrum of Ag-DNA fluorescence, we designed a set of hairpin structures that present homopolymers of each of the four bases in their single-stranded loops (Scheme 1). Results for the Duplex show that the ds stems of the hairpins should not contribute to fluorescence. Instead the fluorescence from hairpin-Ag solutions reflects the interaction of Ag with the bases in the ss loop, allowing a comparison of the relative capacities of C, G, A, and T homopolymers to host fluorescent species.

We find that the attachment of Ag to the four different hairpins results in fluorescence properties that depend strongly on the loop base. C-loop and G-loop solutions exhibit fluorescence of similar brightness (Fig. 2b and d). A-loop solutions fluoresce weakly, peaking at Λ_{ex} = (471.0 ± 0.6) nm, Λ_{em} = (534.9 ± 2.8) nm, with peak intensity less than 1/10th that of C- and G-loop (Supporting Information). T-loop solutions produce no fluorescence for excitation at visible wavelengths.[22] Apparently single-stranded T and A bases have low affinities for fluorescent Ag clusters, which suggests that the attached Ag atoms may bind to A-loop and T-loop primarily on their ds stems. Interestingly, C-loop and G-loop, the hairpins that yield brightest fluores-

ADVANCED MATERIALS

cence, bind fewer Ag atoms than do A-loop and T-loop (Fig. 1 and Supporting Information). One possible explanation is that prior to reduction, charge repulsion and strand deformation from Ag^+ bound to C and G bases in the loops inhibit the binding of Ag^+ ions to the ds stem.

Comparison of the fluorescence spectra of C-Strand and G-Strand (Fig. 2a and c) to those of C-loop and G-loop (Fig. 2b and d) indicates that secondary structure influences the yield of fluorescent species. The primary fluorescence peak for C-Strand is roughly three times brighter than for C-loop and the primary fluorescence peak for G-Strand is roughly five times brighter than for G-loop, despite the identical numbers of each base in C-Strand and C-loop and in G-Strand and G-loop. Apparently the geometrical constraints enforced by the hairpin loop make Ag incorporation more difficult, in agreement with the mass spectra (Fig. 1), which show lower $<N_{Ag}>$ for C-loop and G-loop than for C-Strand and G-Strand.

The fluorescence spectra of the hairpins and Strands also indicate that secondary structure affects fluorescence wavelengths. For C-loop and C-Strand, and G-loop and G-Strand, we expect similar modes of Ag binding to ss bases, with spectral shifts arising from the geometrical constraints imposed by the hairpins. The peak emission and excitation wavelengths for G-loop are red-shifted by roughly 40 nm relative to G-Strand (Fig. 2c and d). This may be due to slight differences in Ag bond lengths and angles, in analogy to the shifts in fluorescence wavelengths observed for Ag clusters embedded in different registrations relative to a noble gas matrix.[23] In contrast, the peak excitation and emission wavelengths for C-loop and C-Strand (Fig. 2a and b) are similar, perhaps because of smaller changes in base stacking associated with the smaller size of cytosine than guanine.

Comparison of the mass and fluorescence spectra provides rough constraints on the number of Ag atoms in the dominant fluorescent species. From the mass spectra, we calculated the fraction, f_N, comprised by species with N_{Ag} = 0, 1, 2, ..., and from the fluorescence spectra we calculated the integrated intensity, I_{Int}, over the main fluorescence peak. Assuming that a single mode of Ag binding predominates for each number, N, of Ag bound to the DNA, we expect the ratio I_{Int}(C-loop)/I_{Int}(C-Strand) to be similar to the ratio f_N(C–loop)/f_N(C-Strand) for the value of N that corresponds to the dominant fluorescent species; and similarly for G-loop and G-Strand. The fluorescence spectra give I_{Int}(C-loop)/I_{Int}(C-Strand) = 0.27 and I_{Int}(G-loop)/I_{Int}(G-Strand) = 0.24. The most similar mass fraction ratios are f_N(C-loop)/f_N(C-Strand) = 0.78, 0.26, and 0.27 for N_{Ag} = 2, 3, and 4; and f_N(G-loop)/f_N(G-Strand) = 0.63, and 0.14 for N_{Ag} = 2 and 3. For all other numbers of attached Ag atoms, the f_N ratios were more than a factor of 10 different from the fluorescence intensity ratios. Thus, hosts with two to four attached Ag atoms are the most likely sources for the observed fluorescence. Because few-atom silver clusters in noble gas matrices[24] fluoresce at wavelengths closer to those we observe than do individual silver atoms in the matrix (which emit at shorter wavelengths), we conclude that Ag_2, Ag_3 and Ag_4 clusters are the probable fluorescent Ag-DNA species. Ag_2 and Ag_3 clusters were also identified as likely fluorophores in recent studies of the sequence 5'-CCCCCCCCCCCC-3'.[25]

To determine whether individual DNA-Ag hairpins are bright enough to image, an important issue for potential applications, we dried drops of the solutions onto coverglass and examined the samples under a microscope equipped for epifluorescence and transmission microscopy. Fluorescence was collected for λ_{em} > 510 nm, with excitation centered at λ_{ex} = 475 nm, well away from the excitation peaks of C-loop and G-loop. Even with this inefficient excitation, isolated fluorescent dots were readily apparent, and increased in number under steady excitation, indicating a photoactivation process. In contrast, dried drops of the A-loop solution showed no fluorescent dots.

Figure 3a shows an image of the fluorescent dots formed by the dried G-loop solution. Results for C-loop were qualitatively similar. Slight defocusing revealed far-field dipole radiation patterns[26] (Fig. 3b) whose orientation did not change even as the isolated emitters fluctuated in intensity. Transmission images in bright field (Fig. 3c; green light) show scattering in the vicinity of the fluorescent dots and transmission images taken through cross-polarizers (Fig. 3d) reveal that birefringence accompanies the scattering. Apparently the DNA-Ag fluorophores are embedded in small salt crystals, likely the birefringent salt $NaNO_3$.[27] Dimmer, more rapidly bleaching fluorescent dots were also present without associated scattering in transmission. Thus protection of the DNA-Ag species by an embedding medium enhances stability and brightness. Recent experiments on Ag nanoclusters bound to the DNA oligomer 5'-CCCCCCCCCCCC-3' and embedded in a polyvinyl alcohol (PVA) film found fluores-

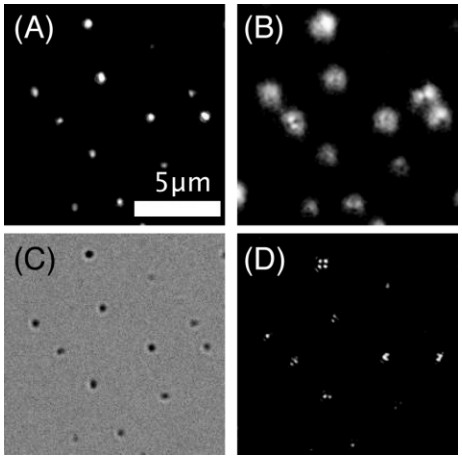

Figure 3. Optical microscopy of a dried drop of the G-loop solution. a) Fluorescence, showing isolated emissive dots (different distances from the focal plane produce variation in apparent size). b) Defocused fluorescence, showing fixed, dipolar emission patterns characteristic of single emitters. c) Transmission of green light showing scattering in the neighborhood of the fluorescent dots. d) Transmission of green light through crossed polarizers, showing birefringence in the neighborhood of the fluorescent dots. Transmission images (c), (d) indicate that individual emitters shown in fluorescence (a), (b) are embedded in small salt crystals.

cence from single emitters bound to this non-hairpin sequence.[25] We have observed fluorescence from single hairpin-Ag emitters embedded in PVA, and, as expected for this homogeneous embedding medium, no light scattering in the neighborhood of the fluorescent dots. For dried and for PVA-embedded Ag-DNA fluorophores, we find stable emission over many weeks. Thus, encapsulation removes the slow fluorescence decay found in aqueous solution.

The dipolar emission patterns (Fig. 3b) and the strong, abrupt variations in intensity (Supporting Information) from the immobilized DNA hairpin-Ag fluorphores are characteristic of individual organic molecules[28] and quantum dots[29] that respond as single quantum systems to environmental fluctuations. We conclude that the isolated fluorescent spots are emission from single emitters; thus, individual DNA hairpin-Ag fluorophores are bright enough to image in standard epi-fluorescence spectroscopy.

In conclusion, we have found that few-atom Ag clusters attached to single-stranded DNA exhibit visible fluorescence with spectral properties that are sensitive to the sequence and secondary structure of the bases that comprise the strand. Isolated, hairpin-based fluorophores exhibit fluorescence with steady dipole radiation patterns and intermittency. These observations are promising for achieving precise placement onto DNA arrays of nanoscale, DNA-based optical elements with sequence-programmed properties.

Experimental

Materials and Synthesis: All strands were purchased from Integrated DNA Technologies with standard desalting and used without further purification. The strands were hydrated in ammonium acetate (80 mM) to 50 μM concentration, heated to 98 °C, and cooled slowly to favor folding into the structure of lowest free energy. To synthesize optically functional Ag-DNA species, we added $AgNO_3$ (0.56 mM) in a 1:2 volume ratio and incubated the solutions for one hour at 4 °C, then reduced them with $NaBH_4$ (1.12 mM) that had been held at 4 °C for 1 hour after mixing. DNA-Ag solutions were stored at 4 °C between measurements.

Characterization: Fluorescence spectra were measured at room temperature in a 1 cm cuvette (Varian Cary Eclipse fluorimeter). Mass spectra were measured using an Applied Biosystems PE SciEx Qstar quadrupole time-of-flight mass spectrometer in negative ion mode at a capillary voltage of –2.0 kV. We mixed the samples with 17 % methanol immediately before measuring mass spectra, to promote desolvation. (This did not significantly affect fluorescence spectra.) Images of single emitters were taken using an Olympus IX-70 microscope fitted with a DVC 1310 CCD camera (full gain, zero offset and 333 ms exposure), with fluorescence collected via a 505 nm long-pass dichroic mirror and a 510 nm long-pass filter. Samples were illuminated with a 100 W mercury arc lamp, through a (475 ± 20) nm bandpass filter. Single emitters were easily visible by eye through the microscope.

Received: September 19, 2007
Revised: November 2, 2007
Published online: January 3, 2008

[1] N.C. Seeman, P. S. Lukeman, *Rep. Prog. Phys.* **2005**, *68*, 237.
[2] C. Lin, Y. Liu, S. Rinker, H. Yan, *ChemPhysChem* **2006**, *7*, 1641.
[3] J. Zheng, P. E. Constantinou, C. Micheel, P. Alivsatos, R. A. Kiehl, N. C. Seeman, *Nano Lett.* **2006**, *6*, 1502.
[4] Y. Y. Pinto, J. D. Le, N. C. Seeman, K. Musier-Forsyth, T. A. Taton, R. A. Kiehl, *Nano Lett.* **2005**, *5*, 2399.
[5] K. Lund, Y. Liu, S. Lindsay, H. Yan, *J. Am. Chem. Soc.* **2005**, *127*, 17606.
[6] H. Yan, S. H. Park, G. Finkelstein, J. H. Reif, T. H. LaBean, *Science* **2003**, *301*, 1882.
[7] S. H. Park, P. Yin, Y. Liu, J. H. Reif, T. H. LaBean, H. Yan, *Nano Lett.* **2005**, *5*, 729.
[8] C. X. Lin, Y. Liu, H. Yan, *Nano Lett.* **2007**, *7*, 507.
[9] S. H. Park, C. Pistol, S. J. Ahn, J. H. Reif, A. R. Lebeck, C. Dwyer, T. H. LaBean, *Angew. Chem. Int. Ed.* **2006**, *45*, 735.
[10] P. W. K. Rothemund, *Nature* **2006**, *440*, 297.
[11] J. T. Petty, J. Zheng, N. V. Hud, R. M. Dickson, *J. Am. Chem. Soc.* **2004**, *126*, 5207. The oligomer studied was 5'-AGGTCGCCGCCC-3'.
[12] T_M were calculated using "OligoAnalyzer", https://www.idtdna.com/analyzer/Applications/OligoAnalyzer (0.040 M salt). Calculations use nearest-neighbor thermodynamic parameters from H. T. Allawi, J. SantaLucia, Jr., *Biochemistry* **1997**, *36*, 10581. T_M were 61, 62, 61, and 63 °C for C-, G-, T-, and A-loop, respectively; 25 °C for C-Strand, 36 °C for G-Strand, and 62 °C for the Duplex.
[13] T_M of annealed hairpins were measured as the peak of dA_{260}/dT, where A_{260} is the 260 nm absorbance. T_M = (59.5 ± 0.1) °C, (61.3 ± 0.3) °C, (63.2 ± 0.1) °C, and (59.7 ± 0.2) °C for C-, G-, T-, and A-loop, respectively.
[14] C-Strand is 5'-TATCCGTC$_5$ATAGGCA-3' and G-Strand is 5'-TGCCTATG$_5$ACGGATA-3'. Hairpins are 5'-TATCCGTX$_5$ACGGATA-3', with X = C, G, A, and T for C-, G-, A-, and T-loop, respectively.
[15] DNA concentrations assume the manufacturer's quoted yield, found from A_{260} measured after desalting (i.e., on random coil sequences) and from a calculated extinction coefficient, as described in the Technical Bulletin *Oligonucleotide Yield, Resuspension and Storage* at https://www.idtdna.com/ (accessed November 2007).
[16] The wavelength of the surface plasmon is sensitive to surface conditions as well as to particle size. S. D. Solomon, M. Bahadory, A. V. Jeyarajasingam, S. A. Rutkowsky, C. Boritz, L. Mulfinger, *J. Chem. Ed.* **2007**, *84*, 322, describe Ag nanoparticles synthesized by $NaBH_4$ reduction of $AgNO_3$ solutions, as in our work.
[17] As evidenced, for example, by the separation of m_{Na}/Z between Na adduct peaks in the charge Z spectrum, where m_{Na} is the mass of the Na atom. The presence of dimers of the DNA strands would have resulted in an additional peaks spaced by $m_{Na}/2Z$.
[18] H. Arakawa, J. F. Neault, H. A. Tajmir-Riahl, *Biophys. J.* **2001**, *81*, 1580. These calf thymus DNA studies found additional binding of Ag^+ within C-G and A-T base pairs for ratios, $R > 0.2$, of Ag^+ per nucleotide. The Duplex's higher G-C content should delay the onset of this additional binding mode to $R > 0.3$, well above the $R = 0.15$ used with the Duplex in our work.
[19] W. Lesniak, A. U. Bielinska, K. Sun, K. W. Janczak, X. Y. Shi, J. R. Baker, L. P. Balogh, *Nano Lett.* **2005**, *5*, 2123.
[20] J. Zhang, S. Xu, E. Kumacheva, *Adv. Mater.* **2005**, *17*, 2336.
[21] Z. Shen, H. Duan, H. Frey, *Adv. Mater.* **2007**, *19*, 349.
[22] Ag-DNA solutions of all the oligomers exhibited weak fluorescence under uv excitation, peaking near λ_{ex} = 310 nm, λ_{em} = 410 nm, and 10–100 times dimmer that the peak fluorescence under visible excitation for all the ss oligomers except T-loop and A-loop.
[23] I. Rabin, W. Schulze, G. Ertl, C. Felix, C. Sieber, W. Harbich, J. Buttet, *Chem. Phys. Lett.* **2000**, *320*, 59.
[24] S. Federigo, W. Harbich, J. Buttet, *J. Chem. Phys.* **1993**, *99*, 5712.
[25] T. Vosch, Y. Antoku, J.-C Hsiang, C. I. Richards, J. I. Gonzales, R. M. Dickson, *Proc. Natl. Acad. Sci. USA* **2007**, *104*, 12616.
[26] M. Böhmer, J. Enderlein, *J. Opt. Soc. Am. B* **2003**, *20*, 554.
[27] M. Wakaki, Y. Komachi, H. Machida, H. Kobayashi, *Appl. Opt.* **1996**, *35*, 2591.
[28] M. F. Garcia-Parajo, G. M. J. Segers-Nolten, J. A. Veerman, J. Greve, N. F. van Hulst, *Proc. Natl. Acad. Sci. USA* **2000**, *97*, 7237.
[29] M. Nirmal, B. O. Dabbousi, M. G. Bawendi, J. J. Macklin, J. K. Trautman, T. D. Harris, L. E. Brus, *Nature* **1996**, *383*, 802.

